

Supernova Inelastic Neutrino-Nucleus Cross Sections from High-Resolution Electron Scattering Experiments and Shell-Model Calculations

K. Langanke,¹ G. Martínez-Pinedo,^{2,3} P. von Neumann-Cosel,⁴ and A. Richter⁴

¹*Institute for Physics and Astronomy, University of Århus, DK-8000 Århus C, Denmark*

²*Institut d'Estudis Espacials de Catalunya, Edifici Nerus, Gran Capità 2, E-08034 Barcelona, Spain*

³*Institució Catalana de Recerca i Estudis Avançats, Lluís Companys 23, E-08010 Barcelona, Spain*

⁴*Institut für Kernphysik, Technische Universität Darmstadt, 64289 Darmstadt, Germany*

(Dated: February 9, 2020)

Highly precise data on the magnetic dipole strength distributions from the Darmstadt electron linear accelerator for the nuclei ^{50}Ti , ^{52}Cr and ^{54}Fe are dominated by isovector Gamow-Teller-like contributions and can therefore be translated into inelastic total and differential neutral-current neutrino-nucleus cross sections at supernova neutrino energies. The results agree well with large-scale shell-model calculations, validating this model.

PACS numbers: 21.60.Cs, 25.30.Dh, 27.40.+z, 23.40.-s

Knowledge about inelastic neutral-current neutrino-nucleus scattering plays an important role in many astrophysical applications, including r-process nucleosynthesis [1, 2], the synthesis of certain elements like $^{10,11}\text{B}$ and ^{19}F during a supernova explosion by the ν -process [3, 4] or for the detection of supernova neutrinos (e.g. [5]). In particular, inelastic neutrino-nucleus reactions might be relevant to several aspects of supernova physics [6, 7, 8]: *i*) for the neutrino opacities and thermalization during the collapse phase, *ii*) for the revival of the stalled shock in the delayed explosion mechanism, and *iii*) for explosive nucleosynthesis. Although inelastic neutrino-nucleus scattering is not yet considered in supernova simulations, a clear call has been made to determine the relevant neutrino-nucleus cross sections, in particular on nuclei in the iron mass range $A \sim 56$, to overcome this shortcoming [7].

Currently no data for inelastic neutrino-nucleus scattering is available, except for the ground state transition to the $J = 1^+$, $T = 1$ state at an excitation energy $E_x = 15.11$ MeV in ^{12}C [9, 10]. It appears as if the needed inelastic neutrino cross sections for iron-region nuclei have to be evaluated by theoretical models without constraint by data. This manuscript will demonstrate that this is in fact not the case. We show that precision data on the magnetic dipole ($M1$) strength distributions, obtained by inelastic electron scattering, supply to a large extent the required information about the nuclear Gamow-Teller (GT) distribution and hence determine the inelastic neutrino-nucleus cross sections for supernova neutrino energies. We also demonstrate that large-scale shell-model calculations agree quite well with the precision $M1$ data, thus validating the use of such models to determine the required cross sections for nuclei where no data exist, or at the finite-temperature conditions in a supernova. The intimate relation of $M1$ and GT strength has already been exploited before to estimate neutrino cross sections for either individual transitions (e.g. in ^{12}C [11, 12]) or total cross sections (e.g. in ^{208}Pb [13]).

The $M1$ response is one of the fundamental low-energy excitations of the nucleus. It can be well explored by means of inelastic electron scattering. Such transitions are mediated by the operator

$$\mathcal{O}(M1) = \sqrt{\frac{3}{4\pi}} \sum_k [g_l(k)\mathbf{l}(k) + g_s(k)\mathbf{s}(k)]\mu_N \quad (1)$$

where \mathbf{l} and \mathbf{s} are the orbital and spin angular momentum operators, and the sum runs over all nucleons. The orbital and spin gyromagnetic factors are given by $g_l = 1$, $g_s = 5.586$ for protons and $g_l = 0$, $g_s = -3.826$ for neutrons [14]; μ_N is the nuclear magneton. Using isospin quantum numbers $t_z = \tau_3/2 = \pm 1/2$ for protons and neutrons, respectively, Eq. (1) can be rewritten in isovector and isoscalar parts. Due to a strong cancellation of the g -factors in the isoscalar part, the isovector part dominates. The respective isovector $M1$ operator is given by

$$\mathcal{O}(M1)_{\text{iv}} = \sqrt{\frac{3}{4\pi}} \sum_k [\mathbf{l}(k)t_z(k) + (g_s^p - g_s^n)\mathbf{s}(k)t_z(k)]\mu_N. \quad (2)$$

We note that the spin part of the isovector $M1$ operator is the zero component of the GT operator,

$$\mathcal{O}(GT_0) = \sum_k 2s(k)t_z(k) = \sum_k \sigma(k)t_z(k), \quad (3)$$

however, enhanced by the factor $\sqrt{3/4\pi}(g_s^p - g_s^n)/2 = 2.2993$. On the other hand, inelastic neutrino-nucleus scattering at low energies, where finite momentum transfer corrections can be neglected, is dominated by allowed transitions. The cross section for a transition from an initial nuclear state (i) to a final state (f) is given by [12]

$$\sigma(E_\nu, i \rightarrow f) = \frac{G_F^2}{\pi} (E_\nu - \omega)^2 B(GT) \quad (4)$$

where G_F is the Fermi coupling constant, E_ν is the energy of the scattered neutrino and ω is the difference

between final and initial nuclear energies. Note that for ground state transitions $E_x = \omega$. The nuclear dependence is contained in the $B(GT)$ reduced transition probability between the initial and final nuclear states with angular momenta J_i and J_f , respectively,

$$B(GT) = \frac{g_A^2}{2J_i + 1} |\langle J_f \parallel \sum_k \sigma(k) \mathbf{t}(k) \parallel J_i \rangle|^2, \quad (5)$$

where g_A is the axialvector coupling constant.

Thus, experimental $M1$ data yield the desired GT_0 information, required to determine inelastic neutrino scattering on nuclei at supernova energies, to the extent that the isoscalar and orbital pieces present in the $M1$ operator can be neglected. On general grounds one expects, as stated above, that the isovector component dominates over the isoscalar piece. Furthermore, it is well known that the major strength of the orbital and spin $M1$ responses are energetically well separated in the nucleus. In pf shell nuclei, which are of interest for supernova neutrino-nucleus scattering, the orbital strength is located at excitation energies $E_x \simeq 2$ –4 MeV [15], while the spin $M1$ strength is concentrated between 7 and 11 MeV. A separation of spin and orbital pieces is further facilitated by the fact that the orbital part is strongly related to nuclear deformation [16]. For example, the scissors mode [17], which is the collective orbital $M1$ excitation, has been detected in well-deformed nuclei like ^{56}Fe [18]. Thus one can expect that in spherical nuclei the orbital $M1$ response is not only energetically well separated from the spin part, but also strongly suppressed.

Examples of spherical pf shell nuclei are ^{50}Ti , ^{52}Cr and ^{54}Fe . As these nuclei have also the advantage that precise $M1$ response data exist from high-resolution inelastic electron scattering experiments [19] we have chosen these 3 nuclei for our further investigation. Our strategy now is to show, in a detailed comparison of data and shell model calculations, that the $M1$ data indeed represent the desired GT_0 information in a sufficient approximation to transform them into total and differential neutrino-nucleus cross sections. The needed shell-model calculations have been performed with the state-of-the-art code NATHAN, developed by Caurier [20], and using the KB3G residual interaction [21]. For ^{50}Ti the diagonalizations involved the complete pf shell, while the calculations for ^{52}Cr and ^{54}Fe are done in truncated model spaces, allowing up to 6 and 5 protons and neutrons to be promoted from the lowest $f_{7/2}$ orbital into the other pf shell orbitals, respectively. The $M1$ and GT_0 response functions are calculated with 400 Lanczos iterations for both isospin channels. As customary in shell-model calculations, the spin operator is replaced by an effective operator $\mathbf{s}_{\text{eff}} = 0.75\mathbf{s}$, where the constant is universal for all pf shell nuclei [22].

Experimentally $M1$ data have been determined for the energy intervals 8.5–11.6 MeV in ^{50}Ti (resolving the $M1$

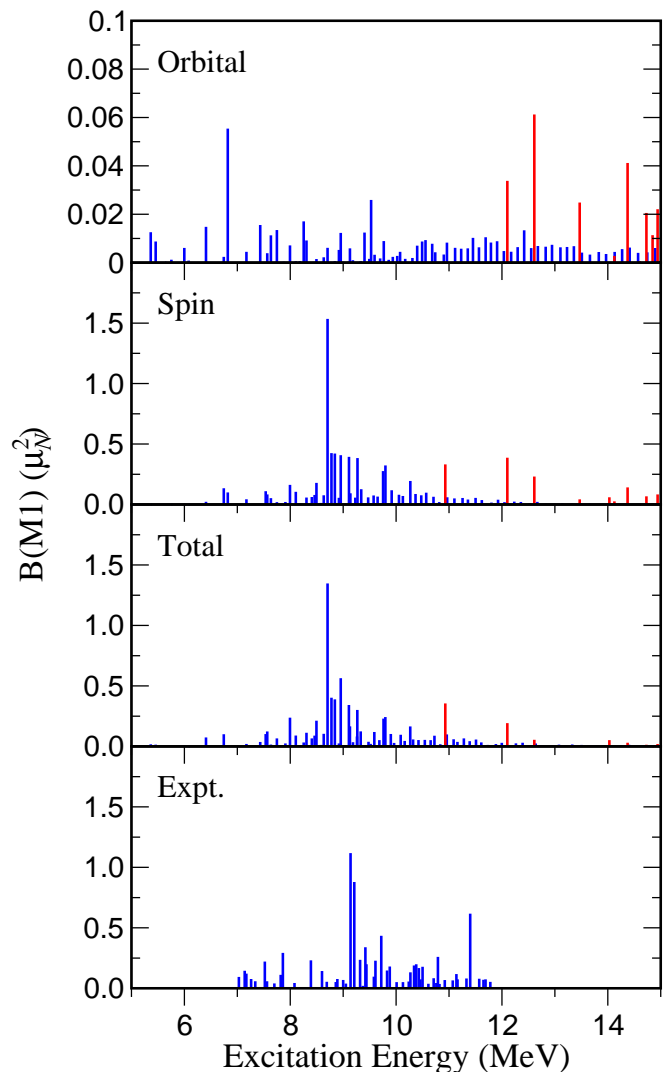


FIG. 1: Comparison of experimental $M1$ strength distribution in ^{52}Cr (bottom) with the shell-model result (third row) and its decomposition into spin (second row) and orbital (top) parts. Note the different scales of the ordinate for the spin and orbital pieces, respectively.

strength for 29 individual states), while for the other two nuclei $M1$ data exist for the energy interval 7.0–11.8 MeV resolving 53 states for ^{52}Cr and 33 states for ^{54}Fe . The summed experimental $B(M1)$ strength (in μ_N^2) in these intervals is 5.4 for ^{50}Ti , 8.7 for ^{52}Cr and 7.5 for ^{54}Fe . For comparison, our shell-model calculations yield total $B(M1)$ strengths of 7.2 for ^{50}Ti , 8.7 for ^{52}Cr and 10.4 for ^{54}Fe . The calculations predict that for ^{52}Cr (^{54}Fe) about 13% (15%) of this strength resides outside of the experimentally investigated energy window, while this value is about 20% for ^{50}Ti . Taking this into account, we find agreement within $\sim 15\%$ between data and calculations. For all nuclei, the energy dependence of the observed $M1$ strength distribution is well reproduced. This is shown in Fig. 1 for the example of ^{52}Cr .

To determine how well the $M1$ data might reflect the desired GT_0 information we have performed shell-model calculations for the individual orbital and spin parts of the $M1$ operator as well as calculations for the GT_0 operator, which, except for a constant factor, represents the isovector spin contribution to the $M1$ operator. The results are displayed in Fig. 1. As expected for spherical nuclei, we observe that the orbital $M1$ strength is significantly smaller, by about an order of magnitude, than the spin $M1$ strength. The interference between the orbital and spin parts is state-dependent and is largely cancelled out, when the strength is averaged over several states. A similar situation occurs for the isoscalar spin contribution, but now its contribution to the total strength is even smaller.

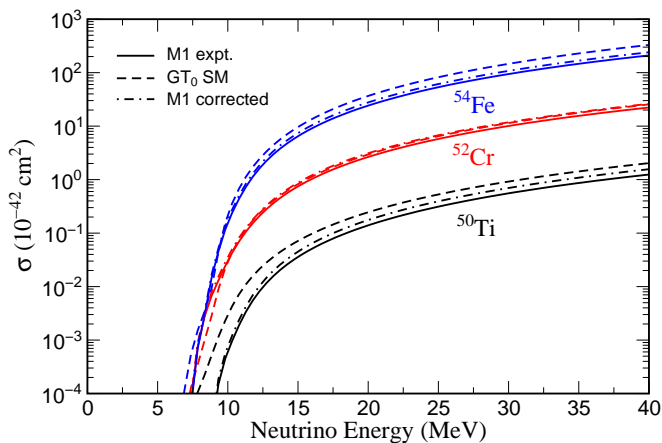


FIG. 2: Neutrino-nucleus cross sections, calculated from the $M1$ data (solid lines) and the shell-model GT_0 distributions (dotted) for ^{50}Ti (multiplied by 0.1), ^{52}Cr , and ^{54}Fe (times 10). The long-dashed lines show the cross sections from the $M1$ data, corrected for possible strength outside the experimental energy window.

Supernova simulations require differential neutrino-nucleus cross sections as functions of initial and final neutrino energies. Neutrinos are modelled in these simulations by multigroup diffusion neutrino transport [23, 24, 25], where neutrinos of different flavors are comprised in energy bins of a few MeV, i.e., cross sections are averaged over many final nuclear states. Cancelling most of the interference between orbital and spin contributions, the $M1$ data should represent the desired GT_0 information, simply using the relation $B(M1) = 3(g_s^p - g_s^n)/(8g_A^2\pi)B(GT)$. Figure 2 compares the total neutrino-nucleus cross sections for the 3 nuclei, calculated from the experimental $M1$ data with those obtained from the shell-model GT_0 distribution. As some of the $M1$ strength is predicted to reside outside of the currently explored experimental energy window (mainly at energies $E^* = 12\text{--}14$ MeV), we have corrected for this by multiplying the “ $M1$ cross section” with the ratio $B(GT_0)/B(GT_0, \Delta E)$, where ΔE defines the exper-

imental energy interval and the ratio is taken from the shell-model calculations. This correction is reasonable for neutrino energies sufficiently larger than 14 MeV. Based on the above theoretical discussion one can assume that the (energetically complete) “ $M1$ cross section” represents the neutrino-nucleus cross sections with an accuracy of 30% (for ^{50}Ti) or better.

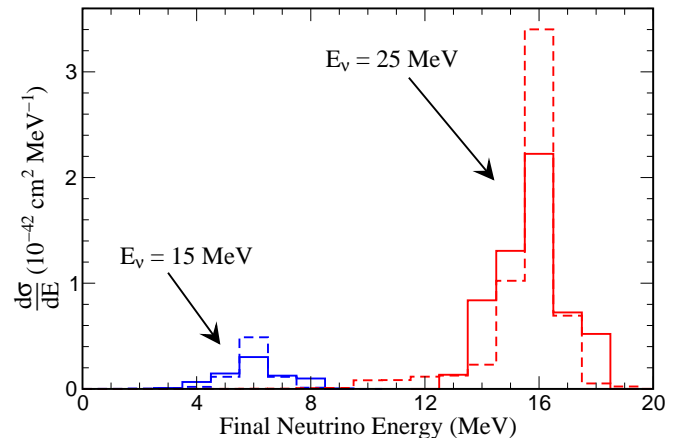


FIG. 3: Differential inelastic neutrino cross sections for ^{52}Cr and initial neutrino energies $E_\nu = 15$ MeV and 25 MeV. The solid histograms are obtained from the $M1$ data, the dashed from shell-model calculations. The final neutrino energies are given by $E_f = E_\nu - \omega$.

Figure 3 shows the differential neutrino cross section for ^{52}Cr at two representative supernova neutrino energies, $E_\nu = 15$ MeV (for ν_e neutrinos) and 25 MeV (ν_μ and ν_τ neutrinos). The cross sections, obtained from the experimental $M1$ data and the shell model, agree quite well, if binned in energy intervals of a resolution (1 MeV or somewhat larger) as required in supernova simulations.

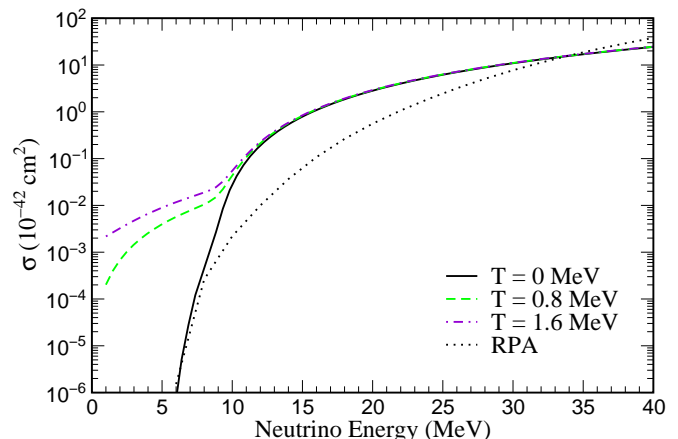


FIG. 4: Inelastic neutrino scattering cross section on ^{52}Cr , calculated on the basis of shell-model GT_0 distributions at finite temperatures. The dotted curve represents the RPA contributions of other multipoles to the cross sections, including finite-momentum transfer corrections.

The comparison of $M1$ and theoretical cross sections suggests that shell-model based calculations of inelastic neutrino scattering at supernova relevant energies are quite accurate and hence the shell model is the method of choice to determine the cross section for the many nuclei in the iron mass region needed in core-collapse simulations. However, such cross sections require additional considerations so far neglected. These must include the effects of finite momentum transfer, of the finite temperature in the supernova environment and the contributions of additional (forbidden) multipoles to the cross section. At supernova energies of interest here (say below 40 MeV) the effect of finite momentum transfer is rather small and leads to a slight reduction (which increases, however, with E_ν) of the cross sections. Adopting the same approach as in [26] we derive the finite-temperature corrections to the cross sections from the GT_0 transitions between a few hundred excited states and the 6 lowest states in ^{52}Cr . The transition strengths are obtained by reversing the shell-model GT_0 matrix elements for these lowest states (using 60 Lanczos iterations per final angular momentum and isospin for the excited states). The results are presented in Fig. 4. Due to the thermal population of excited initial states the neutrino cross sections are significantly enhanced at low energies during the early collapse phase ($E_\nu \sim 10$ MeV). Once the neutrino energy is large enough to allow scattering to the centroid of the GT_0 strength, which resides at energies around 8–11 MeV, finite temperature effects become unimportant and the neutrino cross section can be derived effectively from the ground state distribution, as discussed in [26], and thus is directly constrained by the $M1$ data. This applies to the neutrino energy regime relevant to post-shock supernova simulations.

Contributions to the cross sections from multipoles other than the GT part can be estimated on the basis of the Random Phase Approximation (RPA). These multipoles become only relevant for neutrino energies which are sufficiently larger than the centroid energy of the respective giant resonance of this multipole. At such neutrino energies the cross section depend only on the total strength of the multipole and its approximate centroid energy (both quantities are well described in RPA studies), and not on a detailed reproduction of the strength distribution. Figure 4 displays the RPA contribution to the cross section in ^{52}Cr arising from multipoles other than GT_0 . These become important for $E_\nu > 20$ MeV and dominate for energies higher than 35 MeV.

In summary, we have translated the high-precision (e, e') $M1$ data for ^{50}Ti , ^{52}Cr , and ^{54}Fe , into detailed total and differential inelastic neutral-current neutrino-nucleus cross sections. Besides representing for the first time detailed neutral-current cross sections for nuclei, such data are in particular important for supernova simulations as they allow to constraint theoretical models needed to derive the inelastic neutrino-induced cross sections for the

many nuclei in the medium-mass range present in supernova environment. We have further demonstrated that large-scale shell model calculations are able to describe the data, even in details. Following this validation, shell model calculations for inelastic neutrino cross sections on supernova relevant nuclei are now in progress.

KL is partly supported by the Danish Research Council. GMP is supported by the Spanish MCyT and by the European Union ERDF under contracts AYA2002-04094-C03-02 and AYA2003-06128. PvNC and AR acknowledge support by the DFG under contract SFB 634.

-
- [1] G. M. Fuller and B. S. Meyer, *Astrophys. J.* **453**, 792 (1995).
 - [2] W. C. Haxton, K. Langanke, Y. Z. Qian, and P. Vogel, *Phys. Rev. Lett.* **78**, 2694 (1997).
 - [3] A. Heger, E. Kolbe, W. Haxton, K. Langanke, G. Martínez-Pinedo, and S. E. Woosley (2003), *astro-ph/0307546*.
 - [4] S. E. Woosley, D. H. Hartmann, R. D. Hoffman, and W. C. Haxton, *Astrophys. J.* **356**, 272 (1990).
 - [5] E. Kolbe, K. Langanke, G. Martínez-Pinedo, and P. Vogel, *J. Phys. G: Nucl. Part. Phys.* **29**, 2569 (2003).
 - [6] S. W. Bruenn and W. C. Haxton, *Astrophys. J.* **376**, 678 (1991).
 - [7] W. R. Hix, A. Mezzacappa, O. E. B. Messer, and S. W. Bruenn, *J. Phys. G: Nucl. Part. Phys.* **29**, 2523 (2003).
 - [8] K. Langanke and G. Martínez-Pinedo, *Rev. Mod. Phys.* **75**, 819 (2003).
 - [9] B. Zeitnitz, *Prog. Part. Nucl. Phys.* **32**, 351 (1994).
 - [10] L. B. Auerbach, R. L. Burman, D. O. Caldwell, E. D. Church, J. B. Donahue, A. Fazely, G. T. Garvey, R. M. Gunasingha, R. Imlay, W. C. Louis, et al., *Phys. Rev. C* **64**, 065501 (2001).
 - [11] W. C. Haxton, *Phys. Lett. B* **76**, 165 (1978).
 - [12] T. W. Donnelly and R. P. Peccei, *Phys. Rep.* **50**, 1 (1979).
 - [13] G. M. Fuller, W. C. Haxton, and G. C. McLaughlin, *Phys. Rev. D* **59**, 085005 (1999).
 - [14] P. J. Mohr and B. N. Taylor, *Rev. Mod. Phys.* **72**, 351 (2000).
 - [15] T. Guhr, H. Diesener, A. Richter, C. W. de Jager, H. de Vries, and P. K. A. de Witt Huberts, *Z. Phys. A* **336**, 159 (1990).
 - [16] J. Enders, H. Kaiser, P. von Neumann-Cosel, C. Rangacharyulu, and A. Richter, *Phys. Rev. C* **59**, R1851 (1999).
 - [17] D. Bohle, A. Richter, W. Steffen, A. E. L. Dieperink, N. Lo Iudice, F. Palumbo, and O. Scholten, *Phys. Lett. B* **137**, 27 (1984).
 - [18] R. W. Fearick, G. Hartung, K. Langanke, G. Martínez-Pinedo, P. von Neumann-Cosel, and A. Richter, *Nucl. Phys. A* **727**, 41 (2003).
 - [19] D. I. Sober, B. C. Metsch, W. Knüpfer, G. Eulenberg, G. Kuchler, A. Richter, E. Spamer, and W. Steffen, *Phys. Rev. C* **31**, 2054 (1985).
 - [20] E. Caurier, G. Martínez-Pinedo, F. Nowacki, A. Poves, J. Retamosa, and A. P. Zuker, *Phys. Rev. C* **59**, 2033 (1999).
 - [21] A. Poves, J. Sánchez-Solano, E. Caurier, and F. Nowacki,

- Nucl. Phys. A **694**, 157 (2001).
- [22] P. von Neumann-Cosel, A. Poves, J. Retamosa, and A. Richter, Phys. Lett. B **443**, 1 (1998).
- [23] M. Rampp and H.-T. Janka, Astron. & Astrophys. **396**, 361 (2002).
- [24] A. Burrows, T. Young, P. Pinto, R. Eastman, and T. A. Thompson, Astrophys. J. **539**, 865 (2000).
- [25] M. Liebendörfer, O. E. B. Messer, A. Mezzacappa, S. W. Bruenn, C. Y. Cardall, and F.-K. Thielemann, Astrophys. J. Suppl. **150**, 263 (2004).
- [26] J. M. Sampaio, K. Langanke, G. Martínez-Pinedo, and D. J. Dean, Phys. Lett. B **529**, 19 (2002).